Cell Biochem Biophys (2007) 47:169–177
DOI 10.1007/s12013-007-0001-1

ORIGINAL PAPER

The initial surface composition and topography modulate sphingomyelinase-driven sphingomyelin to ceramide conversion in lipid monolayers

Luisina De Tullio · Bruno Maggio · Steffen Hartel · Jorge Jara · Maria Laura Fanani

Published online: 19 April 2007
© Humana Press Inc. 2007

Abstract Changes of the initial composition and topography of mixed monolayers of Sphingomyelin and Ceramide modulate the degradation of Sphingomyelin by *Bacillus cereus* Sphingomyelinase. The presence of initial lateral phase boundary due to coexisting condensed and expanded phase domains favors the precatalytic steps of the reaction. The amount and quality of the domain lateral interface, defined by the type of boundary undulation, appears as a modulatory supramolecular code which regulates the catalytic efficiency of the enzyme. The long range domain lattice structuring is determined by the Sphingomyelinase activity.

Keywords Phospholipid monolayers · Sphingomyelinase · Epifluorescence microscopy · Sphingomyelin · Ceramide · Phase coexistence · Laterally segregated domains

Luisina De Tullio · B. Maggio · M. L. Fanani (✉)
Departamento de Química Biológica – Centro de Investigaciones en Química Biológica de Córdoba (CIQUIBIC), Facultad de Ciencias Químicas – CONICET, Universidad Nacional de Córdoba, Haya de la Torre y Medina Allende, Ciudad Universitaria, X5000HUA Córdoba, República Argentina
e-mail: lfanani@dqb.fcq.uncor.edu

S. Hartel
Anatomy and Development Biology Program, ICBM Faculty of Medicine, Universidad de Chile, Avda Independencia 1027, Comuna de Independencia, Santiago, Chile

J. Jara
Centro de Estudios Científicos CECS, Universidad Austral de Chile, Independencia 641, Valdivia, Chile

Abbreviations

SMase	Sphingomyelinase
Cer	Ceramide
SM	Sphingomyelin
Pm	Palmitic Acid
dlPC	Dilauroylphosphatidylcholine
DiIC12	1,1'didodecyl-3,3,3′,3′–tetramethylindocarbocyanine
LE	liquid expanded phase
LC	liquid condensed phase

Introduction

Sphingomyelinases (SMase; EC 3.1.4.12) are a group of enzymes that degrade sphingomyelin (SM) to water-insoluble ceramide (Cer) and water-soluble phosphocholine (phosphoryl-trimethyl-ethanolamine). They are widely distributed from bacteria to primates and are classified by their optimal pH, cation requirement and cellular localization [1]. Particularly, *Bacillus cereus* SMase is one of a group of bacterial neutral SMases, Mg^{2+}-dependent [2], which are extra-cellular toxins and exhibit potent hemolytic activity against SM-rich erythrocytes in mammals [1, 3]. It has been suggested that Cer participates in eukaryotic stress response involved in cell differentiation and apoptosis [4, 5]; in model membranes, this lipid induces marked biophysical alterations favoring phase structures of high curvature and formation of phase-segregated domains [6–8]. Recently, enzymaticaly generated Cer-enriched domains were shown to favor apolipoprotein E binding, linking phase segregation events to aterogenesis [9]. To perform their catalytic activity phospholipases such as

Phospholipase C, PI-specific Phospholipase C, Phospholipase A_2 and SMase act associated to the membrane/water interface and their enzymatic activity is modulated by interfacial properties of the membrane substrate in a complex manner in which intermolecular packing, phase state, dipole potential, lipid composition, interfacial curvature, among others factors, are involved [10–18]. It is known that SMase catalytic activity is highly sensitive to subtle changes of the physicochemical conditions of the lipid interface in both monolayer and bilayer systems [15, 17–20]. In this work we studied SMase action using a lipid monolayers system, which allows a continuous control and precise knowledge of the substrate organization and enzyme activity in real time [13, 17, 19, 21–23].

Several studies related ''membrane defects'' (intermolecular packing of non-substrate components as well as phase coexistence) to the activity of lipolytic enzymes [24–27]. In previous publications we have shown by epifluorescence microscopy, using the preferable partition of the fluorescent probe 1,1'didodecyl-3,3,3′,3′ -tetramethylindocarbocyanine ($DiIC_{12}$) into the LE phase of the monolayer, that the real time SMase-driven conversion of SM to Cer generates enzyme-specific changes of topography by forming Cer-enriched domains ranging in size from microns to hundreds of microns [8]. In addition, we have analyzed the succession of discrete morphologic transitions of the Cer-enriched domains. We correlated the time course variations of enzymatic activity to the establishment of defined changes of surface topography taking place at key time periods of the kinetic reaction [28]. In the present work we present how changes in the initial surface topography, brought about by variations of the film composition can determine the time-course, rate, and defined steps of the catalytic activity of *B. cereus* SMase. It is worth remarking that the studies reported in this paper deal with the activity of a secretory soluble neutral SMase of bacterial origin. Even though this enzyme is structurally and functionally related to the mammalian N-SMase family [29], extension of the significance of our results to effect of membrane-bound mammalian SMases, that contribute to the generation of bioactive Cer, is uncertain.

Material and methods

Chemicals

Brain sphingomyelin (SM), brain ceramide (Cer) (obtained from sphingomyelinase-based hydrolysis of brain SM), palmitic acid (Pm) and dilauroylphosphatidylcholine (dlPC) were purchased from Avanti Polar Lipids (Alabaster, AL.) or from Sigma-Aldrich (St. Louis, MO). The (heterogeneous) hydrocarbon moiety of Cer, derived from enzymatic hydrolysis of SM, is the same [30]. The lipophilic fluorescent probe 1,1′-didodecyl-3,3,3′3′-tetramethylindocarbocyanine perchlorate ($DiIC_{12}$) was purchased from Molecular Probes (Eugene, OR). All lipids were over 99% pure by TLC and were used without further purification. *Bacillus cereus* sphingomyelinase (SMase) (EC 3.1.4.12) was obtained from Sigma-Aldrich (St. Louis, MO). NaCl was roasted at 500°C for 4 h. Solvents and chemicals were of the highest commercial purity available. The water was purified by a Milli-Q-system, to yield a product with a resistivity of ~ 18.5 MΩ/cm and absence of surface active impurities routinely checked as described elsewhere [31].

Epifluorescence microscopy of monolayers

All the experiments were carried out in an air conditioned room (22 ± 2°C). The monolayers SM, SM/Cer (9:1), SM/Pm (9:1), SM/dlPC (9:1) doped with 1 mol % $DiIC_{12}$, a fluorescent probe that preferably partitions into liquid-expanded phase [32] were spread from lipid solutions in chloroform/methanol (2:1) over a subphase of 10 mM Tris/HCl, 125 mM NaCl, 3 mM $MgCl_2$, pH 8 until reaching a pressure of less than ~0.5 mN/m [8]. After solvent evaporation (15 min), the monolayer was slowly compressed to the desired surface pressure (π = 10 mN/m). Epifluorescence microscopy (Zeiss Axioplan, Carl Zeiss, Oberkochen, Germany) was carried out using a mercury lamp (HBO 50), a 20X LD objective, a rhodamine filter set, and an all-Teflon zero-order trough (Kibron μ-Trough S; Kibron, Helsinki, Finland) mounted on the microscope stage. Images with exposure times between 40 and 80 μs, were registered with a software-controlled (Metamorph 3.0, Universal Imaging, Union City, CA), charge-coupled device (CCD) camera (Micromax, Princeton Instruments, Downingtown, PA).

Determination of enzymatic activity

The reaction compartment consists of a circular trough (3 ml, 3.14 cm^2) with an adjacent reservoir compartment, connected through a narrow and shallow slit to the substrate monolayer, and an automated surface barostat [17]. The enzymatic reaction (SM → Cer conversion) was followed in real time after the injection of SMase into the subphase compartment (final bulk concentration of 4.8 ng/ml, 1.9 mU/ml). Due to differences in the cross-sectional area between SM (~84 $Å^2$ at 10 mN/m) and Cer (~51 $Å^2$ at 10 mN/m), and because Cer remains at the interface, the enzymatic activity and the different steps of the reaction (lag time, steady-state regime, and slow down-halting of the reaction), can be determined in real time from the reduction of monolayer area at constant surface pressure

(10 mN/m) while the surface barostat replenishes the substrate from a reservoir [8, 17].

Computational analysis of surface topography

Liquid-expanded (LE) and liquid-condensed (LC) lipid phases are presented by bright (high fluorescence/ $DiIC_{12}$-enriched) and dark (low fluorescence/$DiIC_{12}$-depleted) pixels in the 8-bit intensity interval of the fluorescent images (I ε [0,255], 225.5 × 175 μm). A gross segmentation of $DiIC_{12}$-depleted domains was achieved by interactive image processing routines written in IDL (Interactive Data Language, ITT, Boulder, CO) [28]. The definition of Cer-enriched domain borders was optimized by various steps: (i) we increased the number of border positions using β-spline interpolation, (ii) the border positions were used to initiate an active contour model [33]; this model parameterizes internal forces like elasticity (α) or rigidity (β), which counteract line tension or curvature and mimic intrinsic physical properties of a deformable contour, (iii) external force fields were derived from the intensity gradients and laplacians of the original image data by an iterative algorithm based on Generalized Gradient Vector Flows (GGVF) [34]; the vector field iteratively pulls contour points towards the object borders. Force balance between internal and external forces is solved by the Euler-Lagrange condition for the minimization of energy functional E for the parametric curve $\underline{C}(s) = [x(s), y(s)] = \{x_i, y_i\}$, $s \in [0, 1]$:

$$E = \int_0^1 0.5 \cdot [\alpha|\underline{C}'(s)|^2 + \beta|\underline{C}''(s)|^2] + E_{ext}(\underline{C}(s))ds \qquad (1)$$

$\underline{C}'$ and $\underline{C}''$ denominate first and second order derivatives in respect to s. Precise assimilation of the contours towards the morphology of the Cer-enrich domains was archived by setting the appropriate model parameters: α, β, viscosity (γ), external force (k) and number of iterations (t) (see legend to Fig. 2 for illustration). The parameter values were considered to represent the border trajectory with sufficient detail when aprox. 95% of the saturation value is reached; in this condition, independent variations by more than 25% of the parameters did not alter the calculated values by more than 5%. The optimized contours form the basis for the quantitative description of domain morphologies.

Results and discussion

Different SMase kinetic steps are regulated differentially by non-substrate lipids

The activity of SMase against pure SM monolayers shows a latency period (lag time) before exhibiting constant rate catalysis, followed by slow halting of the reaction due to product accumulation at the interface [17, 20].

In previous work we reported that non-substrate lipids (at a mol fraction of 0.1) regulate distinctively SMase action over the different kinetic steps of the enzymatic reaction acting in presence of Ca^{2+}. SMase activity is affected by the product of its own catalytic reaction Cer and, in a surface-mediated cross-talk between phosphohydrolytic reactions, by non-substrate lipids belonging to the Phospholipase A_2 pathway like palmitic acid (Pm) [18]. In this work we reproduced this effect in presence of 3 mM Mg^{2+} where the enzyme is fully active (Table 1). Regarding the surface organization of these films, SM monolayer behave as a LE phase at low surface pressure showing a LE-LC phase transition at ~15 mN/m, Cer and Pm remain highly condensed from about 4 mN/m up to the collapse points at 40 mN/m and 46 mN/m, respectively, and dlPC monolayers show LE phase throughout the whole pressure range. In mixtures of SM with Cer or Pm the mean molecular area of mixed films shows small deviations from ideal behavior and invariance of collapse pressure points, indicating low (if any) miscibility while mixtures of SM with dlPC indicate ideal behavior with full miscibility [8, 20, 35, 36]. Since Cer and Pm favor the precatalytic steps necessary for the enzyme to reach full activity, decreasing the lag time period but inhibiting the rate of activity of SMase during the steady-state kinetic regime (Table 1), there appears to be a correlation between a decrease of the lag time period and a low miscibility of the components in the substrate film. On the other hand, SMase shows very low activity against condensed SM [15, 17, 19] but the inhibition of steady state activity by Cer or Pm can not be attributed to induction of SM condensation because their mixed films with SM follows ideal behavior [35, 36]

The surface topography of substrate monolayers modulates SMase precatalytic steps

A comparison of the surface topography of binary monolayers of substrates and non-substrate lipids at different compositions is shown in Fig. 1. As previously describe [28] the random distribution of domains was ascertained by comparing the frequency distribution of domain centers of enzyme generated or premixed SM-Cer films with the theoretical distribution of a same number of randomly seeded centers. On this basis, it was previously concluded that surface topography actively generated by SMase corresponded to a random distribution during the lag-time period, similar to that of premixed films with an equal proportion of Cer, while it acquired defined lattice superstructuring on entering the kinetic steady-state period.

As previously described [8], the fluorescent probe $DiIC_{12}$ distributes rather uniformly in pure SM films at a

Table 1 Comparison of the enzymatic activity and lag time between pure and mixed monolayers at 10 mN/m. Sphingomyelinase final concentration of 4.8 ng/ml

Lipid monolayer	Enzymatic activity (mol min^{-1}. mm^{-2}) $\times 10^{14}$ ± SEM	Lag time (min)
Pure SM	6.77 ± 0.54	2.50 ± 0.25
SM/Cer (9:1)	3.85 ± 0.58	1.59 ± 0.08
SM/Pm (9:1)	4.73 ± 0.80	1.75 ± 0.05
SM/dlPC (9:1)	7.25 ± 0.13	2.72 ± 0.06

surface pressure of 10 mN/m (some surface defects are seen that represent less than 2% of the surface area, Fig. 1A). However, in premixed film of SM with 10 mol % Cer or Pm there is a random distribution of $DiIC_{12}$-depleted, Cer-enriched domains cover ~ 8% of the surface area for Cer containing films (Fig 1B) and ~ 12% of the surface area for Pm containing films (Fig. 1D). This is in full agreement with the compression isotherm analysis showing negligible miscibility of these components [36]. The mixed monolayer containing SM-dlPC (10 mol %) shows a uniform distribution of $DiIC_{12}$ in a LE phase monolayer (Fig. 1C), in agreement with compression isotherms data.

SMase is reported to degrade more actively SM both in bilayers and monolayers systems when lipids are more loosely packed in a LE phase [15, 17, 19]. From that, we conclude that SMase should be active in the LE phase or, similar to PLA_2 [24], at the lateral interface between the LE continuous phase and the $DiIC_{12}$-depleted domains. The initial presence of lateral interfaces (due to LE-LC phase coexistence) in monolayers composed of SM-Cer or SM-Pm correlates with a reduction of the lag-time thus appearing to shorten some of the required precatalytic steps for SMase. Furthermore, monolayers that initially contain SM-dlPC, do not show initial laterally segregated domains and do not affect SMase lag-time (Fig. 1C and Table 1).

Previous detailed kinetic analysis of the precatalytic steps of the SMase catalytic reaction during the lag time period denoted the existence of second or higher order kinetic steps [20]. Since the end of the lag time correlates with the formation of Cer-enriched domains, as described previously [8, 28], the initial presence of laterally segregated domains may explain the shortening of SMase precatalytic steps, evidenced as a shortening of the lag time period, perhaps increasing the local enzyme concentration at boundary defects due to the lateral interfaces. The presence of surface defects due to phase coexistence, has long been known to activate various phospholipases [12, 24, 37–40].

Comparison of SMase–generated topography from different initial conditions

SMase action was studied against two different monolayers initially containing or not laterally segregated domains. In this work we will focus on the analysis of the differences in the SMase-generated changes in surface topography of a monolayer of initially pure SM or SM-Cer (9:1). Preliminary work shows similar behavior of topography for initial monolayers containing SM-Pm (9:1) (not shown).

In previous work we could establish a direct and reciprocal correlation between the domain morphology and defined catalytic steps of the reaction of SMase acting on monolayers of initially pure SM [8, 28]. In this work, the

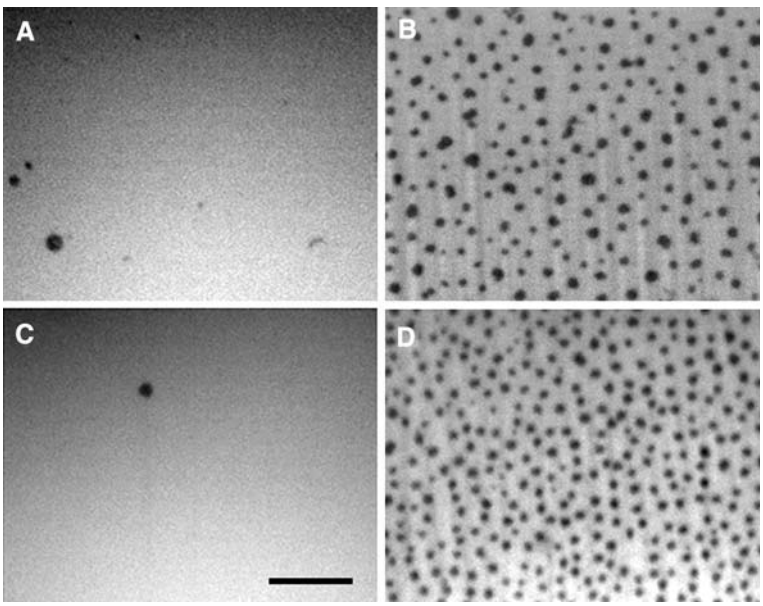

Fig. 1 Fluorescence images of substrate monolayers of different composition. (**A**) pure SM; (**B**) SM/Cer (9:1); (**C**) SM/dlPC (9:1); (**D**) SM/Pm (9:1). Scale bar, 50 μm

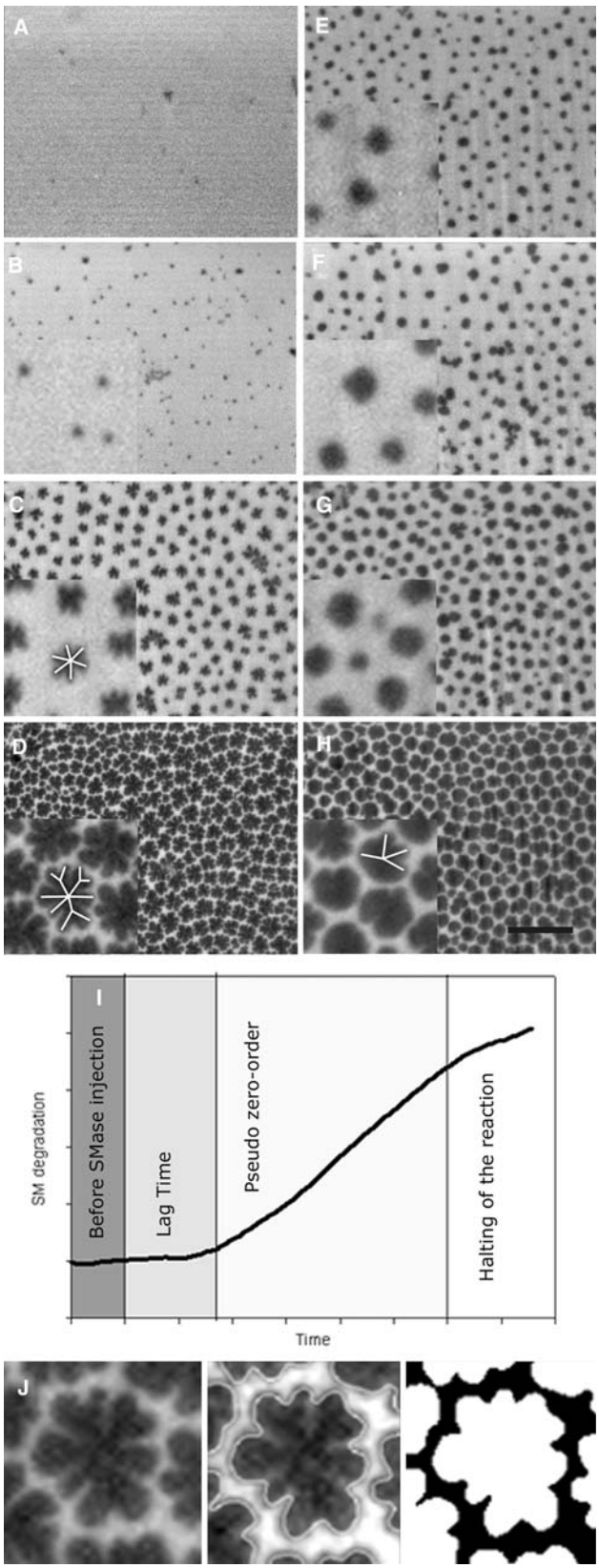

◀**Fig. 2** Topographical properties of SMase driven SM → Cer conversion are defined by the initial substrate monolayer composition. Panels **A**-**H** show representative epifluorescence microscopy image series of the time course of SMase action against pure SM (left) and against premixed films of SM:Cer (9:1) (right). Monolayers are doped by $DiIC_{12}$ (bright regions). Relatives times are t = 0 (**A**, **E**); lag time period (**B**, **F**), early steady state period (**C**, **G**), and late steady state period (**D**, **H**). Scale bar, 50 μm. Inset shows nine-fold amplification of picture sections showing first and second order domain branches. (**I**) Schematic representation of SMase kinetic steps against substrate monolayer. (**J**) Ilustration of Cer-enriched domain border fitted by the Active Contour model (see Materials and methods)

development of an Active Contour model allowed us to perform a detailed analysis of the morphology features of Cer-enriched domains. Figure 2J shows an example of the satisfactory fitting of the domain border achieved by this model, which leads to an accurate calculation of parameters as Circularity and Number of Braches. Even though the assignation of branches by the model can be clearly ascertained, domain morphology analysis has a resolution limit that could lead to an underestimation of the border complexity when the domains are small. Thus the number and complexity of branches structures represent a minimum value. After the injection of SMase under pure SM films, new segregated Cer-enriched domains are rapidly formed at the end of the lag time. Afterwards, during the steady state period, slower nucleation is still present concomitant with growing of the existing domains (Fig. 2A–D and Fig. 3). These domains proceed from circular geometry to branched structures at the beginning of the steady state period (see inset in Figs. 2C, D and 4B, C). By contrast, in the films of SM initially premixed with Cer the number of domains remains almost unchanged throughout the time course while their size grows in approximately circular manner (Figs. 2E–H, 3C, D and 4B, C).

During the steady-state period (while relative substrate excess occurs) there are two main enzymatically-driven transitions of domain morphology occurring in the initially pure SM monolayers namely the change from circular to undulated lipid domains (first and second order domain branching) (inset in Fig. 2C, D) [28]. These boundary-undulated structures are also evident from the analysis of the morphologic parameter Circularity ($perimeter^2$/area) which grows with the progress of the reaction and the Number of Branches per domain which grows up to an average number of ≈7 at the end of the pseudo-zero-order reaction (Fig. 4B, C). If 10 mol % of Cer is present initially at the interface, the SMase activity induces reduced branching of the initially circular domains (circularity ~ 13, almost no branches) to an average of only three

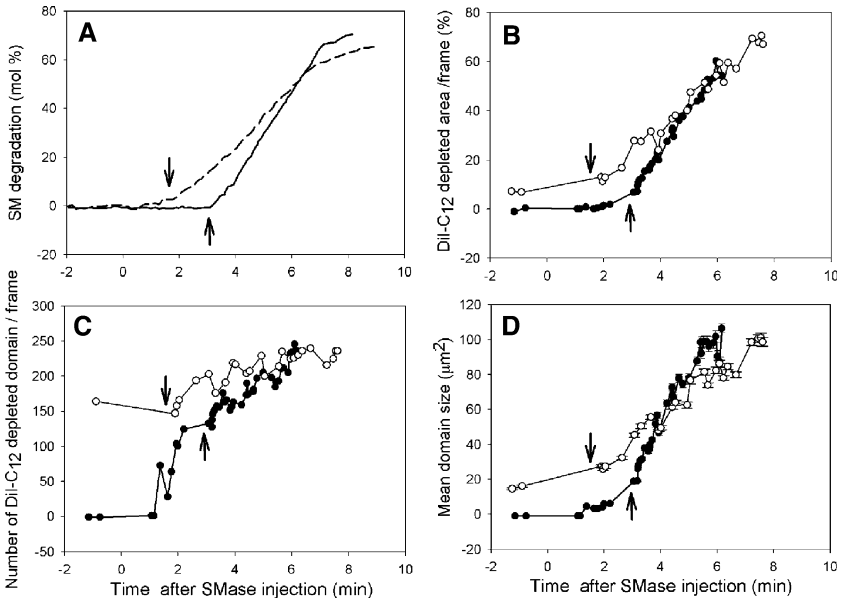

Fig. 3 Comparison of topographic features of substrate-monolayers of different compositions under SMase action as a function of time. (**A**) Time course of the SM to Cer conversion by SMase acting on an initially pure SM monolayer (full line) or premixed SM-Cer (9:1) monolayer (dashed line). Changes in the percentage of $DiIC_{12}$ depleted area per frame (**B**), in the number of $DiIC_{12}$ depleted domains per frame (**C**) and in the average size of $DiIC_{12}$ depleted domains (**D**) are shown as a function of time during SMase-catalyzed SM to Cer conversion. Close circles correspond to initially pure SM monolayers and open circles to initially SM-Cer (9:1) monolayers. The arrows indicate beginning of steady state regime. Parameters in B, C and D were derived by image-processed epifluorescence microscopy from a representative time course reaction, as described in materials and methods. In **D**, error bars represent the SEM for the mean domain size, while in **A**, **B** and **C** figures are absolute numbers

branches per domain at the end of the steady-state period while the circularity remains almost unchanged (Fig. 4B, C). These scarcely undulated structures do not undergo the second order branching that characterizes the progress of the topography of the initially pure SM monolayer under SMase action (see insets in Fig. 2H). All together the data analysis show that an inhibition in enzymatic activity induced by the presence of Cer in the initial monolayer correlates with a decrease of the complexity of domain morphology and, as a consequence, to the quality (curvature) and quantity (total perimeter/frame) of lateral interfaces (Fig. 4). As previously proposed [28], the variations of domain shape appear to represent a topographic code according to which the second order domain branching, occurring at times corresponding to approximately half of the steady-state period, is signaling the maintenance of efficient steady-state catalysis. This probably explains the more efficient catalytic rate for the reaction against initially pure SM monolayers in comparison with SM-Cer (9:1) monolayers.

Changes in the total perimeter (linear amount of the lateral interface per frame) throughout the SMase reaction are a consequence of changes of domain size, domain number and domain border curvature. From Figs. 3 and 4 we can observe that although the SMase reaction against pure SM monolayer shows domain formation as early as 1.5 min, the end of the lag time period is reached at about 3 min and is characterized by the presence in the monolayer of certain amount of perimeter per frame (2000–3000 μm) (Fig. 4A). This is coincident with the amount of perimeter found at the end of the lag time for the reaction against the initially mixed SM/Cer monolayers. This finding supports the above interpretation that the transition from a pre-catalytic enzymatic state to a full catalytic enzyme form strongly depends on the amount of LE-LC lateral interface.

The long range interdomain structure of the interface during the time course of SM degradation against an initially pure SM monolayer, has been described previously to organize in an hexagonal lattice over the late steady state period, different to premixed films with increasing proportions of Cer that do not organize in the same regular manner [8;28]. The initial presence of Cer (10 mol %) does not alter the general lattice topography over the late steady state period, which also shows a marked hexagonal lattice pattern (analysis data not shown). This indicates that the changes of domain morphology depend on the initial presence of laterally segregated Cer-rich domains while the long range domain arrangement follows the pattern specifically determined by the SMase action.

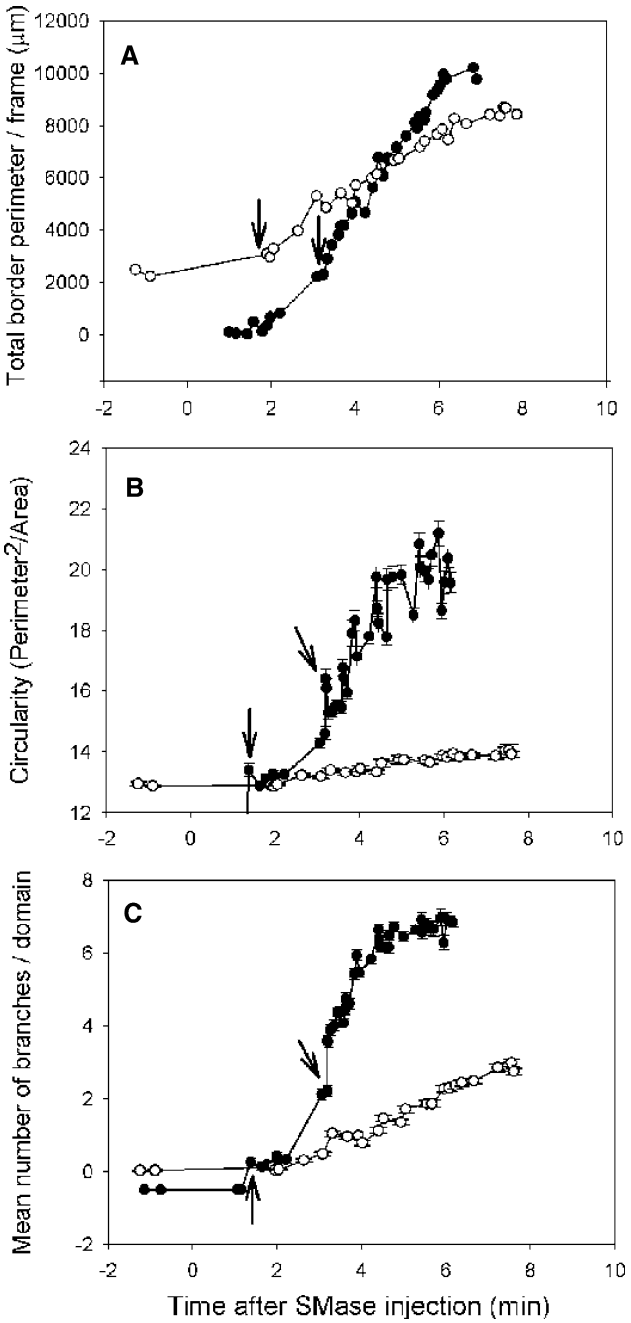

Fig. 4 Comparative morphology analysis of Cer-enriched domains during the time course of SMase reaction. Time-course of the total perimeter per frame, circularity (calculated as the square of the mean perimeter per domain divided by the mean domain area) and average number of branches per domain are shown in panels **A**, **B** and **C** respectively. Close circles correspond to initially pure SM monolayers and open circles to premixed SM-Cer (9:1) monolayers. The arrows indicate beginning of steady state regime. All parameters were derived by image-processed epifluorescence microscopy of a representative time-course reaction, as described in Materials and methods. Error bars represent the SEM for the mean parameters in **B** and **C**, while in **A** figures are absolute numbers

Conclusions

In this article we provide evidences showing that the presence of lateral interfaces due to the LE-LC phase coexistence favors the precatalytic kinetic steps necessary for SMase to enter the steady state kinetic regime. The linear amount and quality of the lateral interface, determined by the boundary undulation and order domain branching of segregated domains, appears as a code controlling SMase catalytic efficiency. This indicates that changes in the initial composition-topography of the interface have the potential to modulate the evolution of the SM to Cer conversion.

Our present results further support directly the role of the membrane topography as a supramolecular modulator of SMase activity in an interactive way, where the formation of laterally segregated domains can affect the kinetic evolution of SM degradation and, conversely and concomitantly the SMase action induces specific structures of laterally segregated membrane domains. Even though the kinetic evolution of domain morphology depends on the initial presence of Cer-rich separated domains, the domain lattice arrangement follows the topography pattern determined by the SMase activity.

It should be taken into account that despite their structural diversity the activity of different types of individual phospholipases has been shown to depend on the variation within a narrow range of a few generic parameters related to the interfacial organization of the substrate [13, 21, 41]. Extending the significance of our results to the effects of membrane-bound Smases, that contribute to the generation of Cer and its biological effects, is uncertain.

However, our studies clearly point out that a further level of SMase regulation can be exerted through variations of composition affecting the surface topography. This may further widen the possibility for exploration of cross-talks and mutual influences among different and simultaneously-acting lipolytic pathways at the membrane surface.

Acknowledgements This work was supported by: SECyT-UNC, CONICET and FONCyT (Argentina); FONDECYT, Empresas CMPC, the Millenium Science Initiative, Fundación Andes and the Tinker Foundation (Chile). L.D. is Doctoral Fellow of FONCYT, B.M. and M.L.F. are Research Investigators of CONICET, S.H. is PI of FONDECYT 1060890 and Jorge Jara was supported by FONDECYT 1030627.

References

1. Goni, F. M., & Alonso, A. (2002). Sphingomyelinases: enzymology and membrane activity. *FEBS Letters, 531*, 38–46.
2. Fujii, S., Itoh, H., Yoshida, A., Higashi, S., Ikezawa, H., & Ikeda, K. (2005). Activation of sphingomyelinase from Bacillus cereus

by Zn2+ hitherto accepted as a strong inhibitor. *Archives of Biochemistry and Biophysics*, *436*, 227–36.
3. Tomita, M., Taguchi, R., & Ikezawa H. (1991). Sphingomyelinase of Bacillus cereus as a bacterial hemolysin. *Journal of Toxicology: Toxin Reviews, 10*, 169–207.
4. Kronke, M. (1999). Biophysics of ceramide signaling: interaction with proteins and phase transition of membranes. *Chemistry and Physics of Lipids*, *101*, 109–21.
5. Hannun, Y. A., & Luberto, C. (2000). Ceramide in the eukaryotic stress response. *Trends in Cell Biology, 10*, 73–80.
6. Maggio, B., Carrer, D. C., Fanani, M. L., Oliveira, R. G., & Rosetti, C. M. (2004). Interfacial behavior of glycosphingolipids and related sphingolipids Curr. *Opinions in Colloid Interface Science, 8*, 448–458.
7. Goni, F. M., & Alonso, A. (2006). Biophysics of sphingolipids I. Membrane properties of sphingosine, ceramides and other simple sphingolipids. *Biochimica Et Biophysica Acta, 1758*, 1902–21.
8. Fanani, M. L., Hartel, S., Oliveira, R. G., & Maggio, B. (2002). Bidirectional control of sphingomyelinase activity and surface topography in lipid monolayers. *Biophysical Journal, 83*, 3416–24.
9. Morita, S. Y., Nakano, M., Sakurai, A., Deharu, Y., Vertut-Doi, A., & Handa, T. (2005). Formation of ceramide-enriched domains in lipid particles enhances the binding of apolipoprotein. E *FEBS Letters, 579*, 1759–64.
10. Kinnunen, P. K., Koiv, A., Lehtonen, J. Y. A., Rytomaa, M., & Mustonen, P. (1994). Lipid dynamic and peripheral interactions of proteins with membranes surfaces. *Chemistry and Physics of Lipids, 73*, 181–207.
11. Boguslavsky, V., Rebecchi, M., Morris, A. J., Jhon, D. Y., Rhee, S. G., & McLaughlin, S. (1994). Effect of monolayer surface pressure on the activities of phosphoinositide-specific phospholipase C-beta 1, -gamma 1, and -delta 1. *Biochemistry, 33*, 3032–7.
12. Maggio, B. (1996). Control by ganglioside GD1a of phospholipase A2 activity through modulation of the lamellar-hexagonal (HII) phase transition. *Molecular Membrane Biology, 13*, 109–12.
13. Maggio, B. (1999). Modulation of phospholipase A2 by electrostatic fields and dipole potential of glycosphingolipids in monolayers. *Journal of Lipid Research, 40*, 930–9.
14. Ahyayauch, H., Villar, A. V., Alonso, A., & Goni, F. M. (2005). Modulation of PI-specific phospholipase C by membrane curvature and molecular order. *Biochemistry, 44*, 11592–600.
15. Ruiz-Arguello, M. B., Veiga, M. P., Arrondo, J. L., Goni, F. M., & Alonso, A. (2002). Sphingomyelinase cleavage of sphingomyelin in pure and mixed lipid membranes. Influence of the physical state of the sphingolipid. *Chemistry and Physics of Lipids, 114*, 11–20.
16. Volwerk, J. J., Filthuth, E., Griffith, O. H., & Jain, M. K. (1994). Phosphatidylinositol-specific phospholipase C from Bacillus cereus at the lipid-water interface: interfacial binding, catalysis, and activation. *Biochemistry, 33*, 3464–74.
17. Fanani, M. L., & Maggio, B. (1997). Mutual modulation of sphingomyelinase and phospholipase A2 activities against mixed lipid monolayers by their lipid intermediates and glycosphingolipids. *Molecular Membrane Biology, 14*, 25–9.
18. Fanani, M. L., & Maggio, B. (1998). Surface pressure-dependent cross-modulation of sphingomyelinase and phospholipase A2 in monolayers. *Lipids, 33*, 1079–87.
19. Jungner, M., Ohvo, H., & Slotte, J. P. (1997). Interfacial regulation of bacterial sphingomyelinase activity. *Biochimica Et Biophysica Acta, 1344*, 230–240.
20. Fanani, M. L., & Maggio, B. (2000). Kinetic steps for the hydrolysis of sphingomyelin by bacillus cereus sphingomyelinase in lipid monolayers. *Journal of Lipid Research, 41*, 1832–40.
21. Bianco, I. D., Fidelio, G. D., & Maggio, B. (1989). Modulation of phospholipase A2 activity by neutral and anionic glycosphingolipids in monolayers. *Biochemical Journal, 258*, 95–9.
22. Bianco, I. D., Fidelio, G. D., & Maggio, B. (1990). Effect of sulfatide and gangliosides on phospholipase C and phospholipase A2 activity. A monolayer study. *Biochimica Et Biophysica Acta, 1026*, 179–85.
23. Ransac, S., Moreau, H., Riviere, C., & Verger, R. (1991). Monolayer techniques for studying phospholipase kinetics. *Methods in Enzymology, 197*, 49–65.
24. Grainger, D. W., Reichert, A., Ringsdorf, H., & Salesse, C. (1990). Hydrolytic action of phospholipase A2 in monolayers in the phase transition region: direct observation of enzyme domain formation using fluorescence microscopy. *Biochimica Et Biophysica Acta, 1023*, 365–79.
25. Muderhwa, J. M., & Brockman, H. L. (1992). Lateral lipid distribution is a major regulator of lipase activity. Implications for lipid-mediated signal transduction. *Journal of Biological Chemistry, 267,* 24184–92.
26. Huang, H. W., Goldberg, E. M., & Zidovetzki, R. (1996). Ceramide induces structural defects into phosphatidylcholine bilayers and activates phospholipase A2. *Biochemical and Biophysical Research Community, 220*, 834–8.
27. Grandbois, M., Clausen-Schaumann, H., & Gaub, H. (1998). Atomic force microscope imaging of phospholipid bilayer degradation by phospholipase A2. *Biophysical Journal, 74*, 2398–404.
28. Hartel, S., Fanani, M. L., & Maggio, B. (2005). Shape transitions and lattice structuring of ceramide-enriched domains generated by sphingomyelinase in lipid monolayers. *Biophysical Journal, 88*, 287–304.
29. Clarke, C. J., & Hannun Y. A. (2006). Neutral sphingomyelinases and nSMase2: Bridging the gaps. *Biochimica Et Biophysica Acta, 1758*, 1893–901.
30. Carrer, D. C., & Maggio, B. (2001). Transduction to self-assembly of molecular geometry and local interactions in mixtures of ceramides and ganglioside GM1. *Biochimica Et Biophysica Acta, 1514*, 87–99.
31. Bianco, I. D., & Maggio, B. (1989). Interactions of Neutral and Anionic Glycosphingolipids with Dilauroylphosphatidylcholine and Dilauroylphosphatidic Acid in Mixed Monolayers. *Colloids and Surfaces, 40*, 249–260.
32. Spink, C. H., Yeager, M. D., & Feigenson, G. W. (1990). Partitioning behavior of indocarbocyanine probes between coexisting gel and fluid phases in model membranes. *Biochimica Et Biophysica Acta, 1023*, 25–33.
33. Kass, M., Witkin, A., & Terzopoulos, D. (1988). Snakes: active contour models. *International Journal of Computer Vision, 1*, 321–331.
34. Xu, C., & Prince, J. L. (1998). Generalized Gradient Vector Flow External Forces for Active Contours Signal Processing.
35. Maggio, B., & Lucy, J. A. (1975). Studies on mixed monolayers of phospholipids and fusogenic lipids. *Biochemical Journal, 149*, 597–608.
36. Fanani, ML. (2001) Supramolecular Modulation of Sphingomyelinase activity in biointerfaces. Ph D. Thesis., Facultad de Ciencias Químicas, Univ. Nacional de Córdoba, Argentina.
37. Basanez, G., Nieva, J. L., Goni, F. M., & Alonso, A. (1996). Origin of the lag period in the phospholipase C cleavage of phospholipids in membranes. Concomitant vesicle aggregation and enzyme activation. *Biochemistry, 35*, 15183–7.
38. Apitz-Castro, R., Jain, M. K., & De Haas, G. H. (1982). Origin of the latency phase during the action of phospholipase A2 on unmodified phosphatidylcholine vesicles. *Biochimica Et Biophysica Acta, 688*, 349–56.

39. Burack, W. R., Yuan, Q., & Biltonen, R. L. (1993). Role of lateral phase separation in the modulation of phospholipase A2 activity. *Biochemistry, 32*, 583–9.
40. Burack, W. R., Dibble, R. G., & Biltonen, R. L. (1997). The relationship between compositional phase separation and vesicle morphology: Implications for the regulation of phospholipase A_2 by membrane structure. *Chemistry and Physics of Lipids, 90*, 87–95.
41. Ransac, S., Deveer, A. M. T. J., & Riviere, C., et al. (1992). Competitive inhibition of lipolytic enzymes. V. A monolayer study using enantiomeric acylamino analogues of phospholipids as potent competitive inhibitors of porcine pancreatic phospholipase A_2. *Biochimica Et Biophysicica Acta, 1123*, 92–100, (Abstract).